JOURNAL OF Materials CHEMISTRY

An optimized route for the preparation of well dispersed supported ruthenium catalysts

Sumeya Bedrane, Claude Descorme* and Daniel Duprez

Laboratoire de Catalyse en Chimie Organique (LACCO), UMR 6503 CNRS, Univeristy of Poitiers, 40 avenue du Recteur Pineau, 86022 Poitiers cedex, France.
E-mail: claude.descorme@univ-poitiers.fr; Tel: 335 49 45 39 97; Fax: 335 49 45 34 99

Received 28th November 2001, Accepted 19th February 2002
First published as an Advance Article on the web 26th March 2002

The preparation of ceria and ceria–zirconia supported ruthenium catalysts was optimized in order to get well-dispersed metal particles. The influence of the preparation method and the treatment conditions on the final morphology of the catalyst was investigated. Ceria-supported catalysts, prepared by incipient wetness impregnation under ultrasound and further treated under pure hydrogen, were shown to have an optimal metal dispersion. In fact, H_2 chemisorption results and TEM observations demonstrated a large increase in the metal accessibility when impregnation was carried out with ultrasound assistance. Ceria-supported ruthenium catalysts with dispersion as high as 60% were prepared.

Introduction

A progressive deterioration of air quality is responsible for most public health and environmental problems. A major contributor to atmospheric pollution is the automobile sector. At the international level, stricter regulations on automotive pollution control are being progressively implemented.

In the case of gasoline-fueled engines, the development of three-way catalysts (TWC) was a major breakthrough. Such systems consist of a temperature-resistant monolith-type structure coated with noble metals impregnated on high surface area supports. Conventional TWCs mostly contain Rh, Pt and/or Pd as the active phase and CeO_2-based oxides as a support dopant. These complex formulations simultaneously need to oxidize both the carbon monoxide (CO) and the unburned hydrocarbons (HC) to CO_2 and to reduce nitrogen oxides (NO_x) to N_2. Optimal performances are obtained if the air-to-fuel ratio remains close to 14.6. This domain around the stoichiometry is called the "operating window". Since the exhaust gas composition strongly oscillates around the stoichiometry under real driving conditions, an oxygen partial pressure "regulator" is required. Oxygen has to be stored during oxygen-rich phases and released when the oxygen partial pressure decreases. Ceria or ceria–zirconia oxides, with a fast Ce^{4+}/Ce^{3+} balance, were shown to be good candidates for oxygen transient storage.

In a recent paper, Descorme *et al.*[1] evidenced the crucial role of activated oxygen species in the whole process of oxygen migration and storage. Dispersed noble metal particles would act as portholes for the subsequent diffusion of oxygen species on the support. The influence of both the nature of the noble metal, the metal particle size and the morphology of the metal/support interface is a major point if one wants to move towards catalytic formulations with faster response times.

It was found that rhodium was the best metal for oxygen activation. Adsorption/desorption of oxygen on Rh surfaces is very fast so that oxygen diffusion and storage is the rate-determining step in the whole process and over a large range of temperature. However, on ceria–zirconia supports, Rh is not good enough as an "activator" for oxygen. In fact, on such oxides oxygen migration is so fast that oxygen activation on the metal particles turns to be the rate determining step in the overall oxygen storage process. For these reasons and in order to find the most reactive system for oxygen activation, Ru was tested as an "activator".

In fact, ruthenium catalysts are used in a number of industrial processes such as ammonia synthesis,[2,3] the Fisher–Tropsch reaction[4–6] and wastewater treatment.[7–9] Furthermore, alumina, silica or zeolite-supported ruthenium catalysts are used in the alkanes hydrogenolysis reaction.[10–14] In that case, ruthenium was found to be more active than any other noble metals (Ru > Rh > Ir > Pt > Pd). Ru catalysts were also used in the CH_4 reforming[15,16] and in the water–gas shift reaction.[17,18] Dealing with automotive pollution control, Zeng and Pang[19] used alumina-supported ruthenium catalysts for N_2O decomposition. High activity was measured at 673 K. Moreover, Sass *et al.*[20] used alumina supported ruthenium catalysts, containing CeO_2, for low-temperature CO oxidation.

Nevertheless, Ru can not be used in TWCs. Temperatures as high as 1273 K can be reached and Ru oxide may form. This oxide is volatile and toxic.

The first step of this long-term investigation concerning oxygen storage was the preparation of well-dispersed Ru-based catalysts. Even though ceria is known to promote noble metal dispersion, ruthenium at the surface of a Ru/CeO_2 catalyst was shown to be poorly dispersed.[8] Depending on the surface area of the ceria supports, authors reported metal particle sizes varying between 7 and 20–30 nm. The maximum dispersion was 14%. One possible reason could be that, Ru crystallizes in a hexagonal structure. This structure could not be adapted for a good dispersion of the Ru on the cubic oxide particles. For the first time, an optimization of the preparation of ceria-supported Ru catalysts is presented. The optimized preparation method will be fully described for ceria-based catalysts and extended to ceria–zirconia mixed oxides. The influence of the preparation parameters and final treatment will be discussed. Concentrating exclusively on the metal dispersion, catalysts were fully characterized by XRD, surface area measurements, TEM direct observations and H_2 chemisorption measurements.

Experimental

Ceria-containing supports (CeO_2 and $Ce_{0.63}Zr_{0.37}O_2$) were directly supplied by Rhodia Electronics and Catalysis (La Rochelle, France) as purely monophasic systems. Before

supply, oxides were pre-calcined at 1173 K for 6 h for stabilization purposes. Surface areas were measured to be 25 and 39 $m^2\ g^{-1}$ for ceria and ceria–zirconia, respectively. The oxide characteristics are summarized in Table 1. The metal precursor $Ru(NO)(NO_3)_3$ was purchased from Strem Chemicals as an aqueous solution (1.5% Ru) packed under argon. Catalysts were prepared by impregnation of the metal solution on the supports. The different preparation procedures will be fully discussed below.

Table 1 CeO_2 and $Ce_{0.63}Zr_{0.37}O_2$ physicochemical characteristics

Oxide	S_{BET}/ $m^2\ g^{-1}$	Structure	Lattice parameter a/Å	Crystallite size/Å
CeO_2	24	Cubic	5.4113	195
$Ce_{0.63}Zr_{0.37}O_2$	39	Cubic	5.3044	66

Catalysts characterization

Specific surface area. Surface areas were measured by N_2 adsorption at 77 K (single-point method) using a Micromeritics Flowsorb II apparatus. Samples (200 mg) were pre-treated at 623 K under 30% N_2 in He (Air Liquide) for 2 h before cooling down to liquid-N_2 temperature (77 K).

Powder X-ray diffraction. XRD patterns were collected on a Siemens D 5005 diffractometer using a copper anode ($\lambda_{K\alpha 1}$ = 1.5406 Å). The apparatus is further equipped with a nickel filter to eliminate the K_β radiation. Diffractograms were acquired between 20–80° 2θ with a step of 0.02° 2θ and an acquisition time of 2 s. Crystalline phases were identified by comparison with ICDD files. To calculate the integrated width (β), diffractograms were simulated using Profile (Socabim, France), assuming a pseudo-Voigt profile for the diffraction peaks. Calculated β values were corrected from the experimental broadening using a LaB_6 reference. The average crystallite size was estimated from the Debye–Sherrer relation [eqn. (1)]

$$d = \frac{\lambda}{\beta \cos\theta} \quad (1)$$

where d is the metal particle size (Å), λ the wavelength (Å), β the corrected full width at half maximum (radian) and θ the Bragg angle (radian).

Electron microscopy. Transmission electron microscopy (TEM) direct observations and energy dispersive X-ray (EDX) analysis were carried out on a CM 120 Philips microscope. In order to obtain a better contrast between the noble metal particles and the support, the samples were pre-reduced at 673 K for 4 h under flowing hydrogen (30 $cm^3\ min^{-1}$). Samples were gently milled, dispersed in ethanol using ultrasound and finally deposited onto carbonated copper grids. Particle size distribution histograms were established from the observation of 500–1000 crystallites on several TEM micrographs. The average particle size was calculated according to eqn. (2)

$$d = \frac{\sum n_i d_i^3}{\sum n_i d_i^2} \quad (2)$$

where n_i is the number of particles whose size is d_i.

Metal dispersions were deduced from TEM observations assuming the particles to be cubic with only five accessible faces. Furthermore, considering that the particles are most probably polycrystalline, an equal distribution at the surface between the (100), (110) and (111) crystallographic faces was also assumed.

H_2 chemisorption experiments

Experiments were carried out in a pulsed chromatographic reactor. Samples (200–250 mg) were introduced in a U-shaped reactor, pre-reduced at 673 K (10 K min^{-1}) under flowing hydrogen (30 $cm^3\ min^{-1}$) for 1 h and outgassed at 673 K under flowing argon (30 $cm^3\ min^{-1}$) for 3 h. Samples were finally cooled under Ar down to the adsorption temperature. High purity H_2 (N55 quality) and Ar (N60 quality) supplied by Air Liquide were used without further treatment. To prevent hydrogen spillover on ceria-containing supports, measurements were carried out at 188 K. Such a method was used by Bernal *et al.*[21,22] and further adapted and optimized to dynamic conditions.[23] In a first sequence, in order to quantify both the reversible and the irreversible chemisorbed hydrogen (H_{C1}), pulses of H_2 (about 5) were injected every 2 min up to full saturation of the sample. After that, the reversibly adsorbed hydrogen is eliminated by flushing the sample with Ar for 10 min. Finally, the only reversible hydrogen adsorption part (H_{C2}) was quantified by pulsing H_2 again on the sample at 188 K. The amount of hydrogen chemisorbed on the noble metal particles is given by: $H_C = H_{C1} - H_{C2}$.

Catalysts preparation

As stated in the Introduction, the goal of the present study was the preparation of well-dispersed ruthenium supported catalysts. For that reason, different preparation routes were evaluated. The experimental conditions for each preparation sequence are fully described in Table 2. A total of seven 1 wt.% Ru/CeO_2 catalysts were prepared and primarily characterized by H_2 chemisorption. The catalysts compositions were checked by elemental chemical analysis (Service Central d'Analyse du CNRS, Solaize, France).

The first catalysts (RC1 and RC2) were prepared by direct impregnation of the ceria support using a $Ru(NO)(NO_3)_3$ aqueous solution. For the synthesis of 2 g of catalyst, 6 g of a $Ru(NO)(NO_3)_3$ solution, containing 0.02 g of Ru, were added to 1.98 g of CeO_2 (100 μmol of Ru g^{-1} of catalyst). The mixture was stirred overnight and subsequently dried at 393 K for 24 h. Finally, the catalyst was divided into two batches before treatment. The first batch (RC1) was calcined under flowing air (30 $cm^3\ min^{-1}$) at 773 K for 4 h (0.5 K min^{-1}). The second batch (RC2) was reduced under flowing hydrogen

Table 2 Influence of the preparation method on the H_2 uptake for 1 wt.% Ru/CeO_2 catalysts

Catalyst	Precursor	Solvent	Support	Impregnation	Treatment	H_2 uptake[a]	H/Ru
RC1	$Ru(NO)(NO_3)_3$	Water	Ceria	Simple	Calcined	2.3	0.02
RC2	$Ru(NO)(NO_3)_3$	Water	Ceria	Simple	Reduced	3.6	0.04
RC3	$Ru(NO)(NO_3)_3$	Water	Ceria	Ultrasound	Calcined	5.8	0.06
RC4	$Ru(NO)(NO_3)_3$	Water	Ceria	Ultrasound	Reduced	14.9	0.15
RC5	$Ru(NO)(NO_3)_3$	Water	Pre-reduced ceria	Ultrasound	Calcined	5.3	0.05
RC6	$Ru(NO)(NO_3)_3$	Water + ammonia	Ceria	Ultrasound	Calcined	4.9	0.05
RC7	$Ru(NO)(NO_3)_3$	Water + ammonia	Ceria	Ultrasound	Reduced	13.2	0.13

[a]μmol H atoms.g^{-1} catalyst from H_2 chemisorption experiments.

(30 cm^3 min^{-1}) at 773 K for 4 h (0.5 K min^{-1}). In fact, it is well known that the nature of the treatment may greatly influence the dispersion of the metallic phase, depending on the stability of the metal under oxidizing or reducing conditions.

For an efficient impregnation, a good "physical" contact between the metal precursor and the support is crucial. One of the key parameters to be optimized was the way the two phases (liquid/solid) are contacted. Ultrasound was used to prevent the oxide particles agglomerating and favor an optimum contact between the metal precursor and the oxide grains surface. RC3 and RC4 were prepared under ultrasound (35 KHz) after addition of the $Ru(NO)(NO_3)_3$ aqueous solution (brown) to the ceria support. Impregnation was carried out for 2 h, up to the point when the solution above the catalyst becomes colorless. Finally, the preparation was separated into two batches, dried at 393 K for 24 h and further calcined (RC3) or reduced (RC4) at 773 K for 4 h.

A second key parameter would be the quality of the "chemical" interaction between the metal complex and the oxide surface. For that reason, the surface chemical modification upon specific pretreatment may favor the anchoring of the metal precursor, chemical bonding at the oxide surface, *etc*. In fact, metal complexes need to be "anchored" to the support for the impregnation to be effective. Interactions may take place *via* hydroxyl groups, structural defects or coordinatively unsaturated sites. Considering the fifth preparation, ceria was pre-reduced under H_2 for 2 h at 573 K (30 cm^3 min^{-1}) to increase the number of oxygen vacancies and/or defects in the oxide support. Impregnation was subsequently carried out under ultrasound. The catalyst (RC5) was dried and calcined at 773 K.

Additionally, the isoelectric point of ceria was obtained for a pH of 6.75. Consequently, cation exchange would be favored in a basic media, when the ceria surface is negatively charged. The pH of the $Ru(NO)(NO_3)_3$ aqueous solution was measured to be 1. For the impregnation to occur in a basic media, a few droplets of ammonia were added to increase the pH up to 10. Impregnation also took place under ultrasound. After drying at 393 K, the sample was divided into two batches. The first batch (RC6) was calcined at 773 K for 4 h while the second batch (RC7) was reduced.

Results and discussion

According to the main goal of this work, the metal accessibility was systematically quantified after each preparation and used as a criteria for the *a posteriori* selection of the preparation conditions.

At first, the samples were characterized by hydrogen chemisorption. The hydrogen uptakes for all the catalysts are summarized in Table 2. It clearly appears that the H_2 consumption is very low.

In fact, it was earlier reported that dynamic methods for hydrogen chemisorption measurements are not suitable for characterizing supported ruthenium catalysts. In fact, H_2 adsorption on Ru was shown to be an activated process. Upon H_2 adsorption, several hours are required before equilibrium is reached. For example, Kubicka[24] carried out volumetric H_2 chemisorption experiments at 293 K and allowed 30–40 min before measuring the equilibrium pressure. Unfortunately, despite this precaution, discrepancies between H_2 chemisorption and X-ray diffraction results were still observed. Nevertheless, Dalla Betta[25] demonstrated the validity of the H_2 adsorption technique when associated with electron microscopy observations, for the measurement of Ru surface areas. While adsorption was negligible after 200 min at 294 K, the authors showed that adsorption–desorption isotherms could be measured overnight. Ru particle sizes calculated from such experiments were in excellent agreement with the results obtained from electron microscopy. In the same way, Goodwin Jr. and Yang[26,27] evidenced that a period of 4–5 h was required to reach equilibrium at room temperature. Considering that H_2 adsorption is faster at higher temperature, Taylor[28] carried out experiments at 373 K with 30 min equilibration after each dose. More recently, Uner *et al.*[29] reported an optimized volumetric H_2 chemisorption method, decreasing the equilibration time to 10 min at 330–360 K. Their results were in agreement with ^1H NMR spectrometry results.

However, such approaches could not be used in our case because of H_2 spillover occurring onto the ceria support. In fact, it is well known that, in the presence of metal particles, ceria may be reduced, even at ambient temperature.[30,31] For the same reasons, O_2 chemisorption or O_2 titration of chemisorbed hydrogen could not be used.[32] Use of other probe molecules such as CO[27,33] or N_2O[34] was also ruled out because of the active role of ceria in the CO oxidation and the NO_x reduction reactions.

Therefore, H_2 chemisorption data reported in the following section are only qualitative. Nevertheless, all measurements were carried out under the exact same conditions so that the results may be used to compare the different Ru catalysts. The higher the H_2 uptake, the better the dispersion.

From the results presented in Table 2, information may be derived about the relative influence of the different preparation parameters: ultrasound, pH control, ceria pre-reduction, final treatment, *etc.*

Effect of the final treatment

The influence of the final treatment may be observed by comparing catalysts RC1 with RC2, both issued from the same preparation. H_2 uptakes are significantly different: 3.6 μmol H atoms g^{-1} catalyst for the reduced catalyst (RC2) compared with 2.3 μmol H atoms g^{-1} catalyst for the calcined one (RC1). Consequently, Ru particles on the reduced catalyst are better dispersed. The same type of conclusion is drawn from the comparisons of RC3 *vs.* RC4 and RC6 *vs.* RC7. This observation is in good agreement with the results reported by Fiedorow *et al.*[35] In fact, in the case of Ru catalysts, a large decrease in the hydrogen uptake was observed when the catalysts were treated under oxygen between 523 and 773 K.

Effect of ultrasound

Comparison between catalysts RC1 and RC3, and RC2 and RC4 demonstrates that the use of ultrasound widely improves the metal dispersion of the metallic phase. H_2 uptake for RC3 and RC4, impregnated under ultrasound, are 2.5 and 4 times as large as for RC1 and RC2, respectively. As a result, the effect of ultrasound assistance clearly appears to have a more pronounced beneficial effect on Ru dispersion compared to the final treatment.

In order to check the exact role of ultrasound, the evolution of the precursor concentration in the solution during impregnation was followed as a function of time. The concentration of the solution was checked by atomic absorption spectroscopy (PerkinElmer 3300 spectrometer). 0.4 cm^3 were taken from the solution above the catalyst and diluted in 25 cm^3 water. The results are reported in Fig. 1.

In the case of catalysts RC3 and RC4, when the preparation is carried out with ultrasound assistance, impregnation is fast. Looking at the evolution of the concentration of the metal precursor in the solution during the preparation of RC3 and RC4, a rapid decrease is observed at the very beginning of the impregnation process. After 1 h, the concentration in $Ru(NO)(NO_3)_3$ tends to zero, indicating that almost all the ruthenium complex has disappeared from the solution. At the same time the solution turns colorless. However, during RC1 and RC2 preparation, the metal precursor concentration

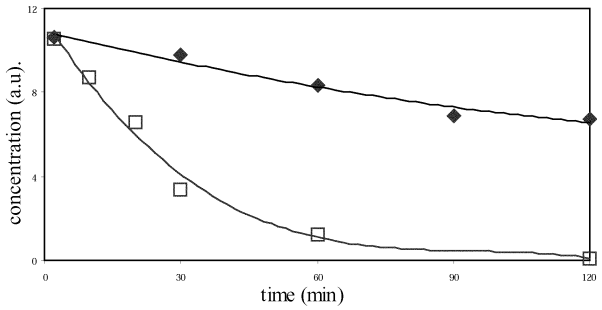

Fig. 1 Evolution of the metal salt precursor concentration during the impregnation (◆ impregnation without ultrasound, □ impregnation under ultrasound).

slowly decreases with time. After 2 h, the Ru precursor concentration only decreases by 40%.

In both cases, The evolution of the concentration as a function of time $C(t)$ might be represented using the following eqn. (3).

$$C = C_0 \times \exp(-at) \quad (3)$$

Parameter "$-a$" corresponds to the initial slope of the curve and gives a measure of the kinetics of ruthenium exchange on the support. From the experimental curves, the evolution of the concentration could be modeled using eqn. (4) for RC1, RC2 and eqn. (5) for RC3 and RC4.

$$C(t) = 10.73 \times \exp(-0.0042 \times t) \quad (4)$$

$$C(t) = 11.55 \times \exp(-0.0399 \times t) \quad (5)$$

From these results, one could conclude that impregnation is about 10 times faster with ultrasound assistance.

Effect of ceria pre-reduction

From the comparison of samples RC3 *vs.* RC5 (for RC5 the ceria was pre-reduced), it is obvious that the pre-reduction of ceria (2 h at 573 K) has only a slight effect on the final dispersion of ruthenium (5.3 *vs.* 5.8 μmol H atoms g^{-1} catalyst for RC5 and RC3, respectively). This result could be explained by a rapid filling of the surface vacancies created upon reduction, just before impregnation, as the ceria support is dispersed into water, or at the very beginning of the impregnation, when the metal precursor is added to the ceria suspension.

Effect of ammonia addition

Finally, comparison of RC6 *vs.* RC3 and RC7 *vs.* RC4 (RC6 and RC7 were prepared using ammonia) demonstrates that the addition of ammonia prior to impregnation for the basification of the solution does not lead to an improvement of the ruthenium dispersion.

In conclusion, catalyst RC4, prepared by impregnation of the ceria support with an aqueous solution of $Ru(NO)(NO_3)_3$ with ultrasound assistance and subsequently reduced at 773 K for 4 h, exhibits the optimum metal dispersion.

This optimum preparation route was extended to $Ce_xZr_{1-x}O_2$ mixed oxides supported catalysts. $Ru/Ce_xZr_{1-x}O_2$ was prepared by addition of an aqueous solution of $Ru(NO)(NO_3)_3$ to the ceria–zirconia support. Impregnation was carried out for 2 h under ultrasound. After drying (24 h at 393 K), the catalyst was reduced under flowing hydrogen (30 cm^3 min^{-1}) for 4 h at 773 K (0.5 K min^{-1}). Both Ru/CeO_2 and $Ru/Ce_xZr_{1-x}O_2$ catalysts were characterized using X-ray diffraction and TEM observations. The main physicochemical characteristics of these two solids are reported in Table 3.

X-ray diffraction did not allow any characterization of the ruthenium particles. Experimental XRD patterns corresponded to those of the oxides alone. No diffraction peak, characteristic of the metal, could be observed in the diffractograms. In fact, Ru particles would be smaller in size than the detection threshold of the apparatus (about 50 Å).

Table 3 Ru/CeO_2 and $Ru/Ce_xZr_{1-x}O_2$ catalysts structural characteristics

Catalyst	$S_{BET}/m^2\ g^{-1}$	H/Ru[a]	d_{TEM}[b]/Å	D[c](%)
Ru/CeO_2	24	0.15	19	60
$Ru/Ce_{0.63}Zr_{0.37}O_2$	37	0.22	13	82

[a]From H_2 chemisorption experiments. [b]Particle size estimated from TEM micrographs. [c]Metal dispersion deduced from d_{TEM}.

To overcome this problem, TEM was used for direct observations of the samples. Two micrographs, representative of Ru/CeO_2 and $Ru/Ce_{0.63}Zr_{0.37}O_2$ are presented in Fig. 2.

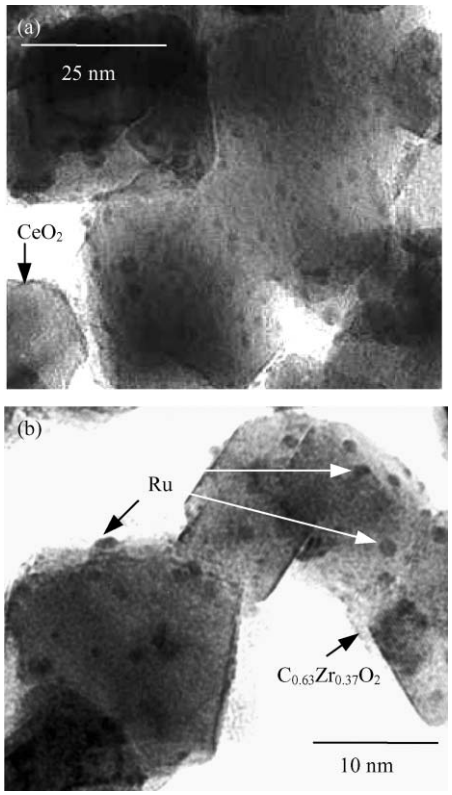

Fig. 2 TEM micrographs for Ru/CeO_2 (a) and $Ru/Ce_{0.63}Zr_{0.37}O_2$ (b).

For Ru/CeO_2, the particle size distribution (Fig. 3) was established from 5 different TEM micrographs corresponding to a total of about 1400 Ru particles. The distribution in size appeared to be very narrow. The average particle size was estimated to be 19 Å, corresponding to a dispersion (D) of about 60%.

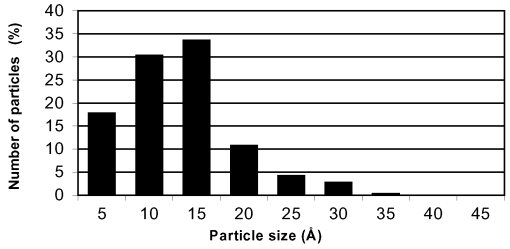

Fig. 3 Particle size distribution for the Ru/CeO_2 catalyst.

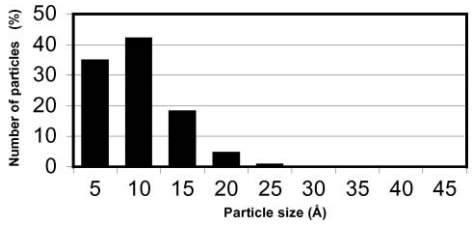

Fig. 4 Particle size distribution for the $Ru/Ce_{0.63}Zr_{0.37}O_2$ catalyst.

For $Ru/Ce_{0.63}Zr_{0.37}O_2$ (Fig. 4), the ruthenium particles were found to be even smaller and the average particle size was 13 Å ($D = 82\%$). An improved dispersion of Ru when supported on ceria–zirconia could simply be attributed to the larger surface area of this support compared to ceria (39 *vs.* 24 $m^2\ g^{-1}$).

Finally, looking at Table 3, a large discrepancy appears between dispersions estimated either from H_2 chemisorption experiments ($100 \times H/Ru$) or from TEM direct observations (D). Dispersions derived from chemisorption measurements were, as a rule, about four times lower than the values deduced from TEM observations. This would confirm, as discussed above, that H_2 chemisorption on Ru is so slow that equilibrium could not be reached, especially at 188 K. Thus, the H_2 consumption would be sharply under-estimated. As a result, information about the absolute dispersion should not be derived from such H_2 chemisorption measurements.

Conclusions

In order to prepare well-dispersed ceria and ceria–zirconia supported ruthenium catalysts, several preparation routes were tested. The influence of both the preparation parameters and the final treatment was checked. A total of seven 1 wt.% Ru/CeO_2 catalysts were prepared.

Systematic H_2 chemisorption measurements showed that a reducing treatment favors high Ru accessibility. Moreover, ultrasound was shown to significantly improve the metal dispersion while the pre-reduction of ceria had only a small effect. Furthermore, ammonia addition for controlling the pH during the impregnation did not lead to any improvement in the Ru dispersion.

The optimal preparation route was shown to be impregnation with ultrasound assistance, using an aqueous solution of $Ru(NO)(NO_3)_3$, followed by a reducing treatment under pure hydrogen at 773 K for 4 h.

The increase of the metal dispersion, when ultrasound was used during the preparation, was attributed to an optimal contact between support particles and the metal precursor. Ultrasound prevents the oxide grains agglomerating and thus favors the metal/support interaction. Finally, improving the metal/support physical interactions during the impregnation leads to better dispersed supported ruthenium catalysts.

References

1 C. Descorme, Y. Madier and D. Duprez, *J. Catal.*, 2000, **196**, 167.
2 O. Hinrichsen, F. Rosowski, M. Muhler and G. Erlt, *Chem. Eng. Sci.*, 1996, **51**, 1683.
3 H. Baris, M. Glinski, J. Kijenski, A. Wokaum and A. Baiker, *Appl. Catal.*, 1986, **28**, 295.
4 M. A. Vannice, *J. Catal.*, 1976, **44**, 152.
5 H. H. Nijs, P. A. Jacobs and J. B. Uytterhoeven, *J. Chem. Soc., Chem. Commun.*, 1979, 10959.
6 L. E. Manzer and K. Kourtakis, *PCT Int. Appl.*, 2000, WO 0010704.
7 V. Felis, C. De Bellefon, P. Fouilloux and D. Schweich, *Appl. Catal. B*, 1999, **20**, 91.
8 L. Oliviero, J. Barbier Jr., D. Duprez, A. Guerrero-Ruiz, B. Bachiller-Baeza and I. Rodriguez-Ramos, *Appl. Catal. B*, 2000, **25**, 267.
9 J. E. Atwater, J. R. Akse, J. O. Thompson and J. A. McKinnis, *Appl. Catal. B*, 1996, **11**, 111.
10 D. J. Sajakowski, J. L. Lee, J. Scwank, Y. Tian and J. G. Goodwin Jr, *J. Catal.*, 1986, **97**, 549.
11 N. M. Gupa, V. S. Kamble and R. M. Iyer, *J. Catal.*, 1984, **88**, 457.
12 S. Gao and L. Schmidt, *J. Catal.*, 1989, **115**, 3546.
13 S. Galvagno, J. Schwank, G. Gubitosa and G. R. Tanszik, *J. Chem. Soc., Faraday Trans. 1*, 1982, **78**, 2509.
14 E. Rodriguez, M. Leconte, J. M. Basset and K. Tanaka, *J. Catal.*, 1989, **119**, 2530.
15 P. Ferreira-Aparicio, I. Rodrigues-Ramos, J. A. Anderson and A. Guerrero-Ruiz, *Appl. Catal. A*, 2000, **202**, 183.
16 U. L. Portugal Jr., C. M. P. Marques, E. C. C. Aranjo, E. V. Morales, M. V. Giotto and J. M. C. Bueno, *Appl. Catal. A*, 2000, **193**, 173.
17 A. Basinska and F. Domka, *Appl. Catal. A*, 1999, **179**, 241.
18 A. Basinska, L. Kopinski and F. Domka, *Appl. Catal. A*, 1999, **183**, 143.
19 H. C. Zeng and X. Y. Pang, *Appl. Catal. B*, 1997, **13**, 113.
20 A. Sass, V. A. Shvets, G. A. Savel'eva, N. M. Popova and V. B. Kazanskii, *Kinet. Katal.*, 1986, **27**(4), 894.
21 S. Bernal, F. J. Botana, J. J. Calvino, M. A. Cauqui, G. A. Cifredo, A. Jobacho, J. M. Pintado and J. M. Rodriguez-Izquierdo, *J. Phys. Chem.*, 1993, **97**, 4118.
22 J. M. Gatica, R. T. Baker, P. Fornasiero, S. Bernal, G. Blanco and J. Kaspar, *J. Phys. Chem. B*, 2000, **104**, 4667.
23 Y. Madier, Ph.D. thesis, Poitiers University, 1999.
24 H. Kubicka, *J. Catal.*, 1968, **12**, 223.
25 R. A. Dalla Betta, *J. Catal.*, 1974, **34**, 57.
26 J. G. Goodwin Jr., *J. Catal.*, 1981, **68**, 227.
27 C.-H. Yang and J. G. Goodwin Jr., *J. Catal.*, 1982, **78**, 182.
28 K. C. Taylor, *J. Catal.*, 1975, **38**, 299.
29 D. O. Uner, M. Pruski and T. S. King, *J. Catal.*, 1995, **156**, 60.
30 L. A. Bruce, M. Hoang, A. E. Hughes and T. W. Turney, *J. Catal.*, 1998, **178**, 84.
31 L. Tournayan, N. R. Marcilio and R. Frety, *Appl. Catal.*, 1991, **78**, 31.
32 D. Duprez, P. Pereira, A. Miloudi and R. Maurel, *J. Catal.*, 1982, **75**, 151.
33 P. Betancourt, A. Rives, R. Hubaut, C. E. Scott and J. Goldwasser, *Appl. Catal. A*, 1998, **170**, 307.
34 H. Berndt and U. Müller, *Appl. Catal. A*, 1999, **180**, 63.
35 R. M. J. Fiedorow, B. S. Chahar and S. E. Wanke, *J. Catal.*, 1978, **51**, 193.